

## Self-Guided Propagation of Ultrashort IR Laser Pulses in Fused Silica

S. Tzortzakis,\* L. Sudrie, M. Franco, B. Prade, and A. Mysyrowicz

*Laboratoire d'Optique Appliquée, CNRS UMR 7639, Ecole Nationale Supérieure de Techniques Avancées-Ecole Polytechnique, Chemin de la Lumière, F-91761 Palaiseau Cedex, France*

A. Couairon† and L. Bergé

*CEA/DAM-Ile de France, Bruyères-le-châtel, France*  
(Received 27 March 2001; published 2 November 2001)

We report self-guided propagation of ultrashort IR laser pulses in fused silica over several Rayleigh lengths. Self-guiding is accompanied by pulse splitting and time compression. Numerical simulations involving pulse self-focusing, temporal dispersion, and multiphoton ionization are found to be in good agreement with the experimental results. They show that a quasidynamic equilibrium between multiphoton ionization and self-focusing drives the filamentation process, while temporal dispersion plays a negligible role.

DOI: 10.1103/PhysRevLett.87.213902

PACS numbers: 42.65.Jx, 42.25.Bs, 42.65.Re, 42.65.Sf

Recently, considerable attention has been paid to the propagation of femtosecond optical pulses in gases. For instance, intense ultrashort infrared (IR) laser pulses propagating through the atmosphere have been shown to self-organize in narrow filaments with high peak intensity about  $10^{13}$  W/cm<sup>2</sup>, which persist over exceptionally long distances [1–7]. This effect results from the dynamical competition between two effects. Because of the nonlinear Kerr response of air, a light beam with input power higher than the self-focusing threshold focuses over a finite distance. The on-axis beam intensity increases through this process, until multiphoton ionization occurs [8]. The ensuing electron plasma defocuses the beam. At powers around critical, the equilibrium between multiphoton ionization (MPI) and Kerr self-focusing (SF) may result in the formation of a long-living solitonlike waveguide [9]. At higher power levels, a dynamic interplay between both processes can sustain the propagation over very long distances [5]. Originally discovered in air [1], such a long-range propagation is not precluded in dense transparent media [10].

Short-scale ( $\sim 1$  mm) filamentation in solids has been observed previously [11] with longer pulses ( $> 10^{-12}$  s). As a consequence, the long pulse duration led to the initiation of important avalanche ionization that permanently damaged the material by a breakdown process and did not allow for the formation of a long-range filament. In contrast, this Letter shows the first detailed observation of self-trapping of IR femtosecond laser pulses in fused silica over long distances (at least 1 cm). We show that the mechanism that balances self-focusing is multiphoton ionization. No significant avalanche contribution is observed in the femtosecond filamentation studied here.

The situation in a dense medium is more complex than in a gas. Besides MPI, other processes must be considered as potential candidates for limiting the collapse of ultrashort pulses. Among them, normal group-velocity dispersion (GVD) is known as promoting pulse splitting, which leads to the sharing of the temporal beam profile into mainly two

symmetric subpulses [12,13]. For example, 90-fs pulses with powers moderately above critical were experimentally observed to split into subpulses in BK7 samples. This splitting process was mainly attributed to GVD [14–16], although in [17] the measured continuum generation and blueshifted spectra suggested a non-negligible role of MPI. In addition, the self-steepening and space-time focusing effects described from deviations to the usual slowly varying envelope approximation [18] may act to shift the beam energy into one of the two pulse edges formed by GVD [19,20]. On the experimental side, there is no report on self-guiding of femtosecond pulses in bulk transparent media, apart from preliminary indications in Ti:sapphire [21] and fused silica [22].

Our measurements include the recording of the beam intensity profile along its propagation axis as well as modifications in the pulse power spectrum, and evolution of the pulse temporal profile using an autocorrelation technique. The experimental results are confronted with direct numerical simulations that account for SF, MPI, avalanche ionization, GVD, self-steepening, and space-time focusing effects, using realistic parameters and initial conditions close to the experiment.

The experimental conditions to obtain the filament are stringent. Formation of the filament occurs when the incident laser power  $P$  exceeds about  $3P_{cr}$ , where in silica glass  $P_{cr} = \lambda_0^2/2\pi n_0 n_2 \approx 2.3$  MW is the critical threshold power for self-focusing, with  $n_0 = 1.453$  being the linear refraction index and  $n_2 = 3.2 \times 10^{-16}$  cm<sup>2</sup>/W the nonlinear refraction index for fused silica. The input pulse duration is 160 fs, and its peak emission wavelength is  $\lambda_0 = 800$  nm. Forming this filament requires an adapted incident laser beam geometry. We use a focusing lens with  $f = 80$  mm, and we situate the entrance face of the silica plate close to the waist of the beam. This positioning is delicate, since a deviation by more than 20% leads to the disappearance of the filament. The high repetition rate of our laser system (200 kHz) presents also a difficulty

for observing filamentation: absorption of even a small amount of energy from every laser shot results in a substantial heating of the sample. This heating, in turn, changes the intrinsic physical properties of the medium and destroys the self-guided mode within a few seconds. To overcome this problem we moved continuously the fused silica plate by means of an  $xy$  motorized stage as shown in Fig. 1a. A self-guided light channel is then produced over a distance exceeding several mm, as shown in Figs. 1b and 1c. The filament size ranges between 10 and 40  $\mu\text{m}$ , which corresponds to maximum intensities of the order of  $10^{13} \text{ W/cm}^2$ , leading to the production of free electrons by multiphoton absorption [23].

The self-guided pulses were characterized as follows. A microscope objective (magnification of  $20\times$ ) coupled to a linear CCD camera recorded the beam intensity profile at different distances along the beam propagation axis (see Fig. 1a). The corresponding laser beam diameters for input energy  $E_{\text{in}} = 2 \mu\text{J}$  are shown in Fig. 1c. Also shown for comparison on the same figure is the linear regime with much lower input energy  $E_{\text{in}} \approx 50 \text{ nJ}$ , for which the laser beam diffracts according to the law of Gaussian optics. In Fig. 1d we present a 3D fluence plot of the filament at the

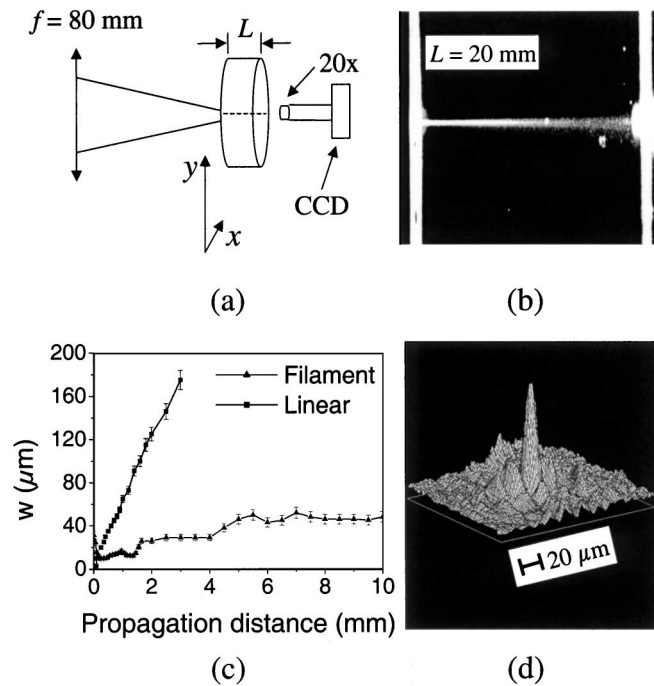


FIG. 1. (a) Experimental procedure for the detection of self-guided filaments in fused silica.  $L = 2, 5, 10 \text{ mm}$  is the thickness of the silica plate. The plate has a continuous planar motion by means of an  $xy$  motorized stage. (b) A transverse photograph of the self-guided filament in fused silica at input energy  $E_{\text{in}} = 2 \mu\text{J}$ . (c) Measured diameter of the filament along its propagation. For comparison the measured linear diffraction regime at low input energy ( $50 \text{ nJ}$ ) is shown. (The 0 of the  $x$  axis corresponds to the entrance face of the fused silica plate.) (d) A 3D fluence plot of the filament at  $2.8 \text{ mm}$  from the entrance window of the silica glass sample.

distance of  $z = 2.8 \text{ mm}$  inside the silica glass. A narrow filament can clearly be observed, surrounded by a light ring structure.

We have also performed measurements of the pulse temporal profile in the filament. For this purpose we used a second harmonic noncollinear autocorrelator with a thin barium borate crystal as a nonlinear medium. The shortest pulse that can be measured with this autocorrelator is of the order of  $30 \text{ fs}$ . The dotted line in Fig. 2a shows the autocorrelation trace of the input laser pulse with duration of about  $160 \text{ fs}$ . After exiting the fused silica plate, the filament propagates in air and diffracts over a distance of  $50 \text{ cm}$ . The central part of the diffracted beam at the exit plane of the sample is introduced in the autocorrelator. The autocorrelation traces of the self-guided pulse at  $2$  and  $5 \text{ mm}$  are shown in Fig. 2a. These autocorrelation traces have a three peak shape, which indicates a pulse splitting of the input laser pulse into mainly two subpulses. This temporal structure stays relatively stable along the filament propagation.

Figure 2b shows the power spectrum of the initial laser pulse, as well as a representative spectrum of the self-guided beam, integrated over about  $100$  shots. The laser beam leaving the  $10\text{-mm}$ -thick sample of fused silica is collected and directed to a  $f = 25 \text{ cm}$  spectrometer equipped with a  $600$  grooves/ $\text{mm}$  diffraction grating and a linear  $16$  bit CCD camera. The entrance slit is set at  $10 \mu\text{m}$ . The power spectrum of the nonlinearly propagating pulse exhibits a broadening which extends over the entire visible spectrum. Less than  $1\%$  of the incident energy is contained in the visible part of the white continuum. As can be seen from Fig. 2b, there is a fringe structure on the self-guided pulse spectrum with an interfringe space of about  $16 \text{ nm}$ . This spectral interval corresponds to the fringe pattern of two ultrashort ( $\sim 60 \text{ fs}$ ) pulses separated by  $120 \text{ fs}$  and is thus compatible with the double-peak pulse structure implied from the autocorrelation traces shown in Fig. 2a.

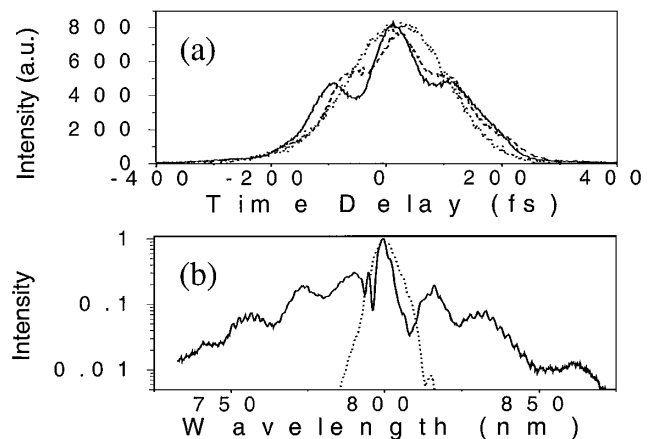


FIG. 2. (a) Measured autocorrelation of the filament at  $2 \text{ mm}$  (solid) and  $5 \text{ mm}$  (dashed), together with that of the initial laser pulse (dotted). (b) Power spectrum of the input pulse (dotted) and that of the filament at  $10 \text{ mm}$  (solid).

We have used a three-dimensional code to simulate the propagation of ultrashort laser pulses in fused silica. The code resolves an extended nonlinear Schrödinger equation, coupled with the density of electrons produced mainly by multiphoton band-to-band transitions. We assume that the beam is linearly polarized with the central frequency  $\omega_0$  ( $\lambda_0 = 800$  nm) and wave number  $k = n_0 k_0$  ( $k_0 = \omega_0/c$ ). The pulse has the radial symmetry and its complex envelope  $\mathcal{E}(r, t, z)$  evolves according to

$$\begin{aligned} \frac{\partial \mathcal{E}}{\partial z} = & \frac{i}{2k} T^{-1} \left( \frac{\partial^2}{\partial r^2} + \frac{1}{r} \frac{\partial}{\partial r} \right) \mathcal{E} \\ & - \frac{ik''}{2} \frac{\partial^2 \mathcal{E}}{\partial \tau^2} + ik_0 n_2 T(|\mathcal{E}|^2 \mathcal{E}) \\ & - \left( \frac{\sigma}{2} + \frac{ik_0}{2\rho_c} \right) T^{-1}(\rho \mathcal{E}) - \frac{\beta^{(K)}}{2} |\mathcal{E}|^{2K-2} \mathcal{E}, \end{aligned} \quad (1)$$

$$\frac{\partial \rho}{\partial \tau} = \sigma_K |\mathcal{E}|^{2K} (\rho_{at} - \rho) + \alpha \rho |\mathcal{E}|^2 - \rho / \tau_r, \quad (2)$$

where  $\tau$  is the retarded time variable  $t - z/v_g$  with group velocity  $v_g$ . The right-hand side of Eq. (1) describes diffraction in the transverse plane, normal GVD with coefficient  $k'' \equiv \partial^2 k / \partial \omega^2|_{\omega_0} = 361$  fs<sup>2</sup>/cm, Kerr self-focusing, plasma absorption with inverse Bremsstrahlung cross section  $\sigma = 2.78 \times 10^{-18}$  cm<sup>2</sup> [5] and defocusing that involve the electron density  $\rho$ , and multiphoton absorption (MPA) with coefficient  $\beta^{(K)} = K \hbar \omega_0 \sigma_K \rho_{at}$ . Connected with these last two quantities,  $\rho_c$  denotes the critical plasma density and  $\rho_{at}$  is the background atom density ( $\rho_{at}/\rho_c \approx 12$  where  $\rho_{at} = 2.1 \times 10^{22}$  atoms/cm<sup>3</sup>). Band-to-band transitions are induced in silica through the gap potential  $U_i = 7.6$  eV [24], yielding the number of photons  $K = 5$  required for ionization. The MPI coefficient then reads as  $\sigma_K = 1.3 \times 10^{-55}$  s<sup>-1</sup> cm<sup>2K</sup>/W<sup>K</sup>. The first term on the right-hand side of Eq. (2) describes the MPI contribution to free electron generation, while the second term accounts for avalanche ionization with  $\alpha = \sigma/n_0^2 U_i$ . The third term represents electron recombination with a characteristic time  $\tau_r \approx 150$  fs in fused silica [23]. In addition, we included, through the operator  $T \equiv 1 + (i/\omega_0) \partial / \partial \tau$ , self-steepening effects with the operator  $T$  in front of the cubic nonlinearity, and space-time focusing with  $T^{-1}$  in front of the transverse Laplacian (see, e.g., Refs. [18,20] for more details).

Equation (1) is solved by means of a Fourier spectral decomposition in time and a standard Crank-Nicholson scheme in space, applied to each spectral component. As initial conditions, we consider input beams lying at the entrance face of the glass sample similarly to the experiment. Those have the standard Gaussian shape with input power  $P_{in}$ , and a waist  $w_0 = 30$   $\mu$ m (measured experimentally). The temporal FWHM pulse length is 160 fs. The results for initial energy  $E_{in} = 2$   $\mu$ J and power  $P_{in} \approx 5P_{cr}$  are shown in Fig. 3. Figure 3(a) displays evidence of

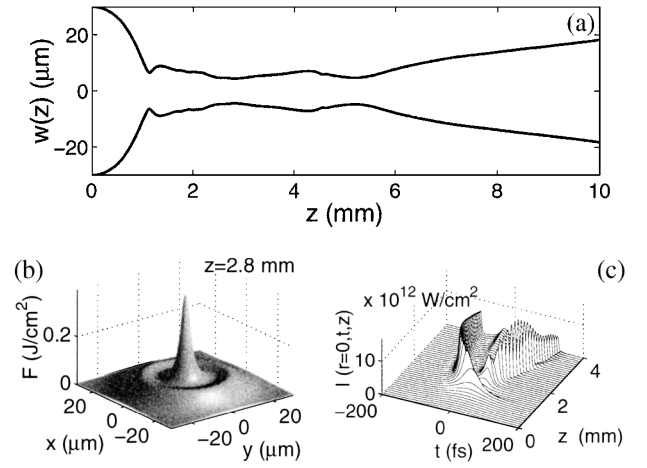


FIG. 3. (a) Calculated diameter of the filament along its propagation. (b) Calculated 3D fluence profile of the filament at 2.8 mm. (c) Temporal profile of the filament along the first 4 mm of propagation.

the emergence of a light channel, having a diameter close to that measured experimentally. Figure 3(b) shows a 3D fluence profile of the filament at a distance of  $z = 2.8$  mm. Note the ring structure that surrounds the filament, in agreement with the experiment (Fig. 1d). Figure 3(c) shows the distortions in the temporal intensity profile of the beam. Two main peaks are formed, which both undergo a sharp steepening. They keep an almost similar distribution over a distance of about 4 mm, while afterwards a more complex multi-peaked structure develops. The longitudinal length of the resulting filament can be estimated from the pulse power,  $P = \int |\mathcal{E}|^2 d\vec{r}$ , which is continuously lost by the filament through MPA mainly. Using  $dP/dz \sim -\beta^{(K)} I_{max}^{K-1} P$  from Eq. (1) yields the filament length  $\Delta z \approx \ln[P_{in}/P(z)] / \beta^{(K)} I_{max}^{K-1}$ . For the numerically computed value  $I_{max} = 1.5 \times 10^{13}$  W/cm<sup>2</sup>, the distance  $\Delta z$  beyond which  $P(z)$  goes below  $P_{cr}$  and prevents further SF is thus  $\Delta z \approx 1$  cm, in agreement with the experimental observation.

For completeness, we also numerically computed the intensity spectra in wavelength and the temporal autocorrelations of the transmitted beam. The latter, detailed in Fig. 4(a), form a three-peaked structure. Keeping in mind that the number of peaks  $\mathcal{N} = 2N - 1$  yields the number of split pulses,  $N$ , one easily infers that two main spikes characterize the temporal profile of the beam. By comparing the experimental (Fig. 2a) and numerical autocorrelations, we can observe their similar aspects at different propagation distances. Figure 4(b) shows the input laser pulse power spectrum, together with the filament spectrum at 10 mm. Again, we can notice the relatively good agreement between the experimental data (Fig. 2b) and the numerical results, even on the satellite spectral components of the filament. Residual spectral discrepancies are most likely due to phase distortions and unavoidable small energy fluctuations in the initial laser pulses, which are

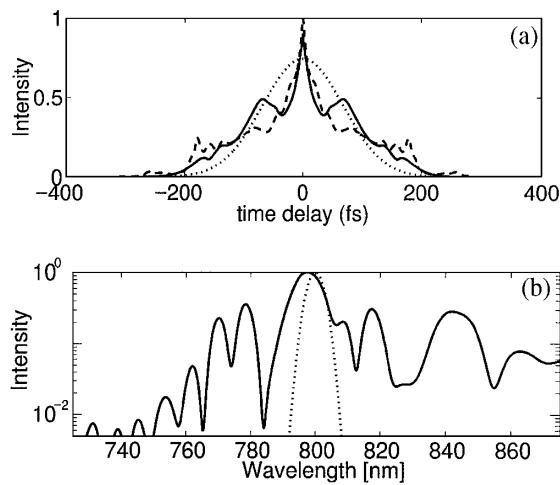


FIG. 4. (a) Calculated autocorrelations: of the initial pulse (dotted), of the filament at 2 mm (solid) and 5 mm (dashed). (b) Power spectra: initial pulse (dotted) and filament (solid) at 10 mm.

not included in our simulations where we introduce ideal Gaussian pulses with flat spectral phase.

Inspection of the simulations brings to light that filament robustness is mainly due to a dynamic balance between MPI and optical Kerr effect. Although they may promote a resembling two-spike temporal profile, group-velocity dispersion, self-steepening and space-time focusing play a secondary role in the present case. To check this point, we performed several simulations, with and without temporal dispersive effects (GVD and/or the operators  $T, T^{-1}$ ). We observed that the action of these terms had no significant influence on the stabilization of the light channel, which is actually promoted by the plasma density alone. This property agrees with the prediction by Henz and Herrmann [10]. However, using a power close to critical, the numerical simulations of Ref. [10] do not show the formation of two pulses.

It is interesting to compare our results to the cases previously explored in Refs. [14–16]. Using different initial conditions (i.e., beam geometry), these authors found a propagation regime in fused silica without long-range channeling, but where pulse splitting occurred. From their model equation omitting MPI, GVD together with self-steepening and space-time focusing were concluded to provide the main mechanism in limiting the self-focusing of ultrashort pulses through the splitting process. Similar regimes led by the interplay between GVD and self-focusing, with plasma generation playing a minor role, were revealed in some of our simulations but for much larger values of the GVD coefficient or larger initial beams [14–16].

In conclusion, we have presented, for the first time, a long-range filamentation in fused silica using femtosecond

IR laser pulses. The self-guided pulse is accompanied by an important spectral broadening and pulse breaking with two or more shorter subpulses. Our numerical simulations reproduce most of the experimental observations. They show that the self-guided filament actually results from the balance between self-focusing and MPI.

We kindly acknowledge the expert assistance of Y.-B. André and G. Hamoniaux.

\*Email address: stzortz@ensta.ensta.fr

†Present address: Centre de Physique Théorique, CNRS UMR 7644, F-91128 Palaiseau Cedex, France.

- [1] A. Braun, G. Korn, X. Liu, D. Du, J. Squier, and G. Mourou, *Opt. Lett.* **20**, 73 (1995).
- [2] E. T. J. Nibbering *et al.*, *Opt. Lett.* **21**, 62 (1996).
- [3] L. Wöste *et al.*, *Laser Optoelektronik* **29**, 51 (1997).
- [4] B. La Fontaine *et al.*, *Phys. Plasmas* **6**, 1615 (1999).
- [5] M. Mlejnek, E. M. Wright, and J. V. Moloney, *Opt. Lett.* **23**, 382 (1998).
- [6] H. R. Lange *et al.*, *Opt. Lett.* **23**, 120 (1998); A. Chiron *et al.*, *Eur. Phys. J. D* **6**, 383 (1999).
- [7] L. Bergé and A. Couairon, *Phys. Plasmas* **7**, 210 (2000).
- [8] L. V. Keldysh, *Sov. Phys. JETP* **20**, 1307 (1965).
- [9] L. Bergé and A. Couairon, *Phys. Rev. Lett.* **86**, 1003 (2001).
- [10] S. Henz and J. Herrmann, *Phys. Rev. A* **59**, 2528 (1999).
- [11] E. Yablonovitch and N. Bloembergen, *Phys. Rev. Lett.* **29**, 907 (1972); R. R. Alfano and S. L. Shapiro, *Phys. Rev. Lett.* **24**, 592 (1970).
- [12] P. Chernev and V. Petrov, *Opt. Lett.* **17**, 172 (1992); J. E. Rothenberg, *ibid.* **17**, 583 (1992).
- [13] V. Tikhonenko, J. Christou, and B. Luther-Davies, *Phys. Rev. Lett.* **76**, 2698 (1996).
- [14] J. K. Ranka, R. W. Schirmer, and A. L. Gaeta, *Phys. Rev. Lett.* **77**, 3783 (1996).
- [15] S. A. Diddams, H. K. Eaton, A. A. Zozulya, and T. S. Clement, *Opt. Lett.* **23**, 379 (1998).
- [16] A. A. Zozulya, S. A. Diddams, A. G. Van Engen, and T. S. Clement, *Phys. Rev. Lett.* **82**, 1430 (1999).
- [17] A. Brodeur and S. L. Chin, *J. Opt. Soc. Am. B* **16**, 637 (1999).
- [18] T. Brabec and F. Krausz, *Phys. Rev. Lett.* **78**, 3282 (1997); *Rev. Mod. Phys.* **72**, 545 (2000).
- [19] J. K. Ranka and A. L. Gaeta, *Opt. Lett.* **23**, 534 (1998).
- [20] A. L. Gaeta, *Phys. Rev. Lett.* **84**, 3582 (2000).
- [21] E. Baubeau, C. Le Blanc, and F. Salin, in *Proceedings of the Conference on Lasers and Electro-Optics, Baltimore, 1997* (Optical Society of America, Washington, DC, 1997), Vol. 11, p. 407.
- [22] I. G. Koprnikov, A. Suda, P. Wang, and K. Midorikawa, *Phys. Rev. Lett.* **84**, 3847 (2000).
- [23] P. Audebert *et al.*, *Phys. Rev. Lett.* **73**, 1990 (1994).
- [24] R. Tohmom, H. Mizuno, Y. Ohki, K. Sasagane, K. Nagasawa, and Y. Hama, *Phys. Rev. B* **39**, 1337 (1989).